New Inflight Calibration of OCO-3's Oxygen A-Band for Build 11 Products

Graziela R. Keller[1*], Robert A. Rosenberg[1], Aronne Merrelli[2], Christopher W. O'Dell[3], Vivienne Payne[1], and Abhishek Chatterjee[1]

1. Jet Propulsion Laboratory, California Institute of Technology, Pasadena, CA USA 91011
2. University of Michigan, Ann Arbor, MI, USA.
3. Colorado State University, Fort Collins, CO, USA

Introduction

The Orbiting Carbon Observatory-3 (OCO-3) instrument, operated from the International Space Station, was launched on May 4th, 2019. Its primary objective is to provide high-precision estimates (< 0.25% of background values) of the column averaged dry-air mole fraction of carbon dioxide (XCO_2) and solar-induced chlorophyll fluorescence (SIF). It consists of three long slit imaging spectrometers that provide high resolution spectra in three infrared channels centered at 0.765 (O_2 A-band), 1.61 (Weak CO_2), and 2.06 µm (Strong CO_2). The shortest wavelength channel is characterized by absorption lines from molecular oxygen and the other two channels show numerous carbon dioxide (CO_2) absorption lines. While the Weak and Strong bands provide independent measurements of CO_2 column abundance, the oxygen A-band is used to constrain optical path length and SIF, and is also used for cloud screening. All three bands are used in the determination of aerosol optical depth.

OCO-3 relies on three tungsten halogen lamps for relative inflight radiometric calibration, which is frequently updated (every three to seven days) through the delivery of inflight gain degradation coefficients. Throughout the mission, OCO-3 has undergone important changes in instrument response. In the A-band, these are associated with the buildup of contaminants, which are removed by periodic decontamination procedures where the focal planes are allowed to warm. One way contaminant buildup affects the A-band in OCO-3 is by imparting a S-like shape to the spectra (something that has not been observed in OCO-2 data), which is inconsistent among observations of the different lamps and between lamps and science observations.

In Build 11, we derive the spectral shape of inflight gain degradation in the A-band from observations of clear ocean scenes, while its magnitude continues to be derived from lamps only.

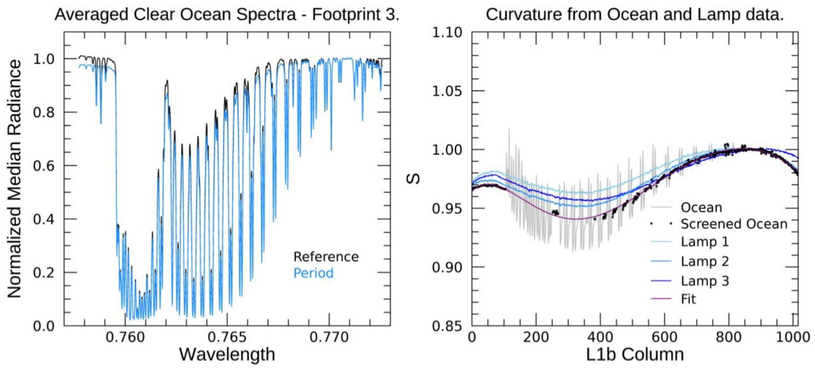

Fig.1. Left: Examples of averaged clear ocean spectra for a period of high contamination (blue - before decontamination event on January 2021) and a reference period of low contamination (black - after the decontamination event). Right: The shape parameter S, derived from ocean and lamp data. The light gray curve is the ratio of the spectra shown on the left panel. Once it is screened to remove residual spectral lines, we are left with the black dots, through which we fit an order 6 polynomial (purple curve).

We define the shape parameter S (Fig.1) to describe curvature

$$S_j(t) = \frac{R_j(t)}{\overline{R}_{j_{start}:j_{end}}(t)} \Big/ \frac{R_{ref\ j}}{\overline{R}_{ref\ j_{start}:j_{end}}}$$

where Rj refers to scene radiance at time t for a given sample j, calibrated with with pre-launch gains only. R is the averaged radiance in the spectral window defined between j_{start} and j_{end}, chosen to be 0.7708 – 0.7710 µm, to match continuum regions in Earth spectra. The subscript ref indicates a reference period of low contamination of the focal planes.

Build 11 Algorithm

- Averaged normalized spectra from thousands of ocean soundings were created for each ARP period with sufficient data.
- Reference periods of low ice contamination were selected for each decontamination cycle.
- From the ratio between the average spectra of each ARP period and reference period, we calculate the shape parameter S throughout the mission.

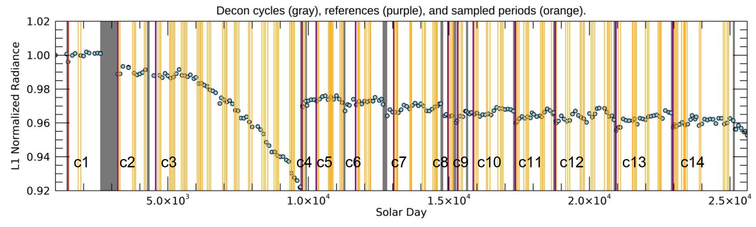

Fig.2. Temporal coverage of clear ocean data (orange lines). Lamp 1 radiances (blue dots) shown for reference.

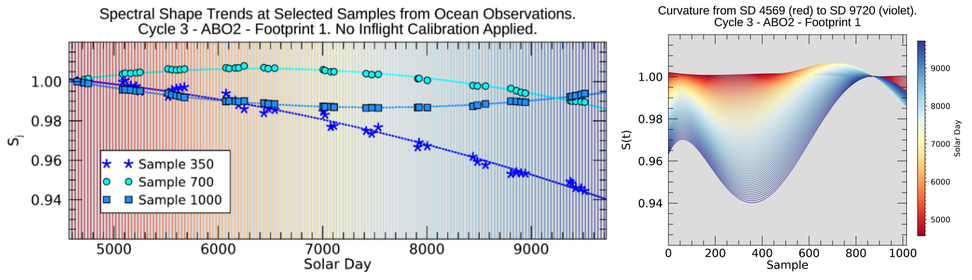

Fig.3. Spectral shape trend in time and best fit curves (left) and resulting shape parameter as a function of spectral sample and time (right) for decontamination cycle 3.

- We fit the data within each decontamination cycle in time, to fill gaps in data coverage. Each spectral sample of each footprint is fit independently.
- These fits were used to produce the curves on the right side panel of Fig.3, such that curvature, with respect to a reference period, can be retrieved for any solar day.
- In Build 11, the spectral shape of the instrument gain degradation is given by the product of the shape parameter S, derived from ocean scenes and the gain degradation coefficient derived from lamp data at the reference period [1,2].

Impact on Product

Spectral Residuals - In Version 10, residuals between science observations and best fit models showed curved spectral profiles during periods of high ice accumulation, that were also inconsistent among footprints. In Version 11, curvature in the residuals was mostly resolved, as seen on Fig. 4.

Empirical Orthogonal Functions (EOFs) - OCO-3's final operational retrievals include the removal of a set of EOFs. EOFs associated with curvature derived from Version 10 products explained up to 9% of the variance, depending on footprint. This dropped to less than 1% in Version 11, where curvature related EOFs also show less footprint dependence.

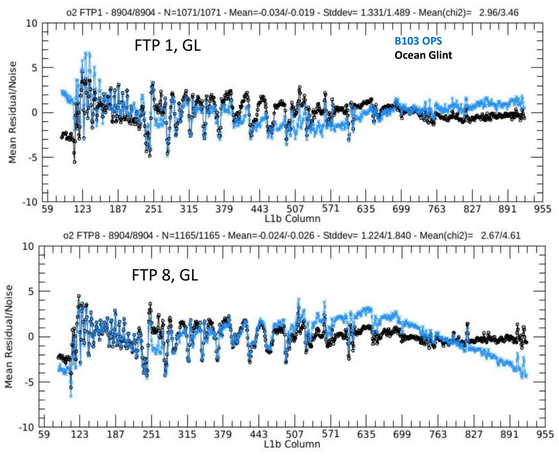

Fig.4. Spectral residuals

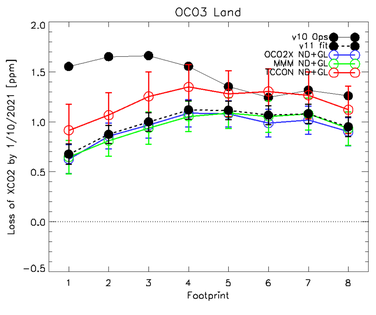

Fig.5. Loss of XCO_2 in Build 10 (black dots with solid line) and Build 11 (black dots with dashed line).

XCO_2 Drift – OCO-3 Version 10 retrievals showed a slow XCO_2 drift during OCO-3's longest decontamination cycle, ending on January 2021, with respect to OCO-2 retrievals, TCCON measurements, and models and required and ad-hoc correction on post processing [4,5]. On Version 11, the loss of XCO_2 was reduced to about 1 ppm or less, as shown on Fig. 5.

Conclusions

The new calibration of the A-band drastically reduced the curvature of spectral residuals between model and science observations, which previously had a strong footprint dependence. In Build 10, this manifested itself in the form of a slow drift of XCO_2, from February 2020 to January 2021, with respect to models, TCCON, and OCO-2, which was corrected during the post-processing step. This correction was necessary, despite the use of Empirical Orthogonal Functions (EOFs) to remove the artifact in Build 10. EOFs associated with curvature derived from Build 10 products explained up to 9 % of the variance. This dropped to less than 1 % in Build 11, where curvature related EOFs are no longer removed. The slow drift in XCO2 was significantly reduced to about 1 ppm or less in Build 11, depending on footprint.

References

1. G. R. Keller et al., "New Inflight Calibration of OCO-3's A-Band for Version 11 Products," in prep.
2. G. R. Keller et al., "Inflight Radiometric Calibration and Performance of the Orbiting Carbon Observatory 3 for Version 10 Products," IEEE Transactions on Geoscience and Remote Sensing, vol. 60, pp. 1–18, 2022.
3. R. Rosenberg et al., "Preflight Radiometric Calibration of Orbiting Carbon Observatory 2," IEEE Transactions on Geoscience and Remote Sensing, vol. 55, no. 4, pp. 1994–2006, 2017.
4. A. Chatterjee et al., "Orbiting Carbon Observatory-3 (oco-3) data quality statement: Level 2 forward and retrospective processing data release 10 (v10 and v10r), v10.4 lite files.
5. T. E. Taylor et al., "Evaluating the Consistency Between OCO-2 and OCO-3 XCO_2 Estimates Derived from the NASA ACOS Version 10 Retrieval Algorithm," Atmospheric Measurement Techniques, vol. 16, no. 12, pp. 3173–3209, 2023.

* OCO-3 Calibration Team Lead
graziela.r.keller.rodrigues@jpl.nasa.gov